Evidence for Watson−Crick and Not Hoogsteen or Wobble Base Pairing in the Selection of Nucleotides for Insertion Opposite Pyrimidines and a Thymine Dimer by Yeast DNA Pol η[†]

Hanshin Hwang and John-Stephen Taylor*

Department of Chemistry, Washington University, St. Louis, Missouri 63130

Received August 13, 2004; Revised Manuscript Received December 16, 2004

ABSTRACT: We have recently reported that pyrene nucleotide is preferentially inserted opposite an abasic site, the 3′-T of a thymine dimer, and most undamaged bases by yeast DNA polymerase η (pol η). Because pyrene is a nonpolar molecule with no H-bonding ability, the unusually high efficiencies of dPMP insertion are ascribed to its superior base stacking ability, and underscore the importance of base stacking in the selection of nucleotides by pol η. To investigate the role of H-bonding and base pair geometry in the selection of nucleotides by pol η, we determined the insertion efficiencies of the base-modified nucleotides 2,6-diaminopurine, 2-aminopurine, 6-chloropurine, and inosine which would make a different number of H-bonds with the template base depending on base pair geometry. Watson−Crick base pairing appears to play an important role in the selection of nucleotide analogues for insertion opposite C and T as evidenced by the decrease in the relative insertion efficiencies with a decrease in the number of Watson−Crick H-bonds and an increase in the number of donor−donor and acceptor−acceptor interactions. The selectivity of nucleotide insertion is greater opposite the 5′-T than the 3′-T of the thymine dimer, in accord with previous work suggesting that the 5′-T is held more rigidly than the 3′-T. Furthermore, insertion of A opposite both Ts of the dimer appears to be mediated by Watson−Crick base pairing and not by Hoogsteen base pairing based on the almost identical insertion efficiencies of A and 7-deaza-A, the latter of which lacks H-bonding capability at N7. The relative efficiencies for insertion of nucleotides that can form Watson−Crick base pairs parallel those for the Klenow fragment, whereas the Klenow fragment more strongly discriminates against mismatches, in accord with its greater shape selectivity. These results underscore the importance of H-bonding and Watson−Crick base pair geometry in the selection of nucleotides by both pol η and the Klenow fragment, and the lesser role of shape selection in insertion by pol η due to its more open and less constrained active site.

It was originally thought that the exceptionally high fidelity of nucleotide insertion by DNA polymerases could be explained solely by H-bonding interactions between the template base and its complementary nucleotide. The 0.2−4 kcal/mol differences in the thermodynamic stabilities between matched and mismatched base pairs in DNA duplexes can at best account for an $\sim 10^3$-fold difference in fidelity, requiring additional explanations for the experimentally observed fidelities of up to 10^6 (*1*−*4*). In one proposal, it was argued that a hydrophobic active site that removes water could amplify the free energy differences between matched and mismatched base pairs by decreasing entropy differences and increasing enthalpy differences (*2*). Additional explanations have focused on geometric selection in the initial binding of a nucleotide, and during a subsequent nucleotide-induced conformational or induced-fit step that leads to phosphodiester bond formation (*5*, *6*). While some have proposed that these steps contribute individually to the overall selectivity in a so-called fidelity check point model, others have argued that one need only consider differences between matched and mismatched base pairs in a rate-limiting bond-forming step (*7*).

Studies with difluorotoluene deoxyribonucleotide (dFTP), a nonpolar analogue of thymidine that cannot form hydrogen bonds, have revealed that geometrical fit may be more important than the H-bonding in the selection of nucleotides by the exo$^-$ Klenow fragment of *Escherichia coli* DNA pol I (*8*, *9*). Despite its inability to make hydrogen bonds, difluorotoluene nucleotide was found to be inserted only ∼40 times less efficiently than thymidine nucleotide opposite A, and with fidelity roughly comparable to that of thymidine nucleotide. On the basis of this study and studies with other nucleotide analogues, a "steric exclusion model" was proposed that emphasizes the importance of steric complementarity of the nascent base pair in the polymerase active site and base stacking with the primer terminus in determining the fidelity of DNA synthesis (*10*). In another testimony to steric fit and base stacking, pyrene nucleotide, a large hydrophobic polycyclic aromatic hydrocarbon of a size comparable to a base pair that is devoid of H-bonding donors and acceptors, is efficiently inserted opposite abasic sites by KF, but not opposite normal bases (*11*).

[†] This work was supported by NIH Grant CA40463 (J.-S.T.).

* To whom correspondence should be addressed: Department of Chemistry, Campus Box 1134, Washington University, One Brookings Drive, St. Louis, MO 63130. Phone: (314) 935-6721. Fax: (314) 935-4481. E-mail: taylor@wustl.edu.

10.1021/bi048244+ CCC: $30.25
Published on Web 03/01/2005

In contrast to the pol A family polymerases, the error prone DNA damage bypass polymerase, pol η,[1] seems to rely more on base stacking and H-bonding than on steric fit alone in selecting nucleotides for insertion as judged by recent results with pyrene (P) and difluorotoluene (F) nucleotides. Unlike the case for KF, pyrene nucleotide is inserted by pol η more efficiently opposite most normal bases than is the complementary nucleotide, presumably due to its superior base stacking ability and size that may be able to trigger the putative conformational change that precedes phosphodiester bond formation (*12*). On the other hand, difluorotoluene deoxynucleotide, which also exhibits very strong base stacking ability (*13*, *14*), but is smaller and may not be able to trigger the conformational change, is more than 200 times less efficiently inserted opposite A than is T by pol η. This suggests that H-bonding may be more important than steric fit in nucleotide selection by pol η (*15*).

Though all evidence to date suggests that pol η selects nucleotides for insertion based on a Watson−Crick base pair geometry, a recently determined crystal structure of the related Y-family polymerase, Dpo4, shows dideoxyadenosine triphosphate in a Hoogsteen base pair with the 5′-T of a cis-syn thymine dimer (*16*). Hoogsteen base pairing has also been observed in a crystal structure of human pol ι between a template A and an incoming dTTP (*17*). Kinetic evidence also suggests that pol ι may preferentially form a wobble base pair between a template T and an incoming dGTP (*18*).

In this paper, we have investigated the importance of H-bonding and base pair geometry in nucleotide selection by pol η by measuring the steady state insertion efficiency of various base-modified triphosphates opposite C, T, and the 3′-T and 5′-T of the cis-syn thymine dimer. We find that nucleotide insertion efficiency is maximal for those nucleotides that can base pair in a Watson−Crick fashion and that have the most hydrogen bonds. By using 7-deazaadenosine triphosphate, we provide evidence that Hoogsteen base pairing is not involved in the insertion of A opposite either of the Ts of the dimer as has been suggested to occur for other DNA damage bypass polymerases. We also demonstrate that the insertion selectivity for pol η parallels that of the Klenow fragment for Watson−Crick-like base pairs, but not for mismatches, emphasizing the importance of H-bonding in nucleotide selection by both polymerases, but greater shape selection by the Klenow fragment.

MATERIALS AND METHODS

Enzymes and Substrates. The catalytic core of yeast pol η with a His_6 tag on its N-terminus was prepared as previously described (*19*). Exo$^-$ Klenow fragment was purchased from New England Biolabs. Standard oligodeoxynucleotides were purchased from IDT and then purified by PAGE purification. Oligodeoxynucleotides containing a site-specific thymine dimer were synthesized on an Expedite 8909 DNA synthesizer utilizing a thymine dimer phosphoramidite building block (*20*, *21*) and then purified on an anion exchange DEAE column and on a C18 column. All DNA primers and templates used in this study are shown in Figure 1B. T4 polynucleotide kinase and [γ-^{32}P]ATP were obtained from Amersham Pharmacia Biotech. Primers were labeled with [γ-^{32}P]ATP and polynucleotide kinase and were annealed with 1.25 equiv of templates by heating at 95 °C for 5 min and cooling over several hours.

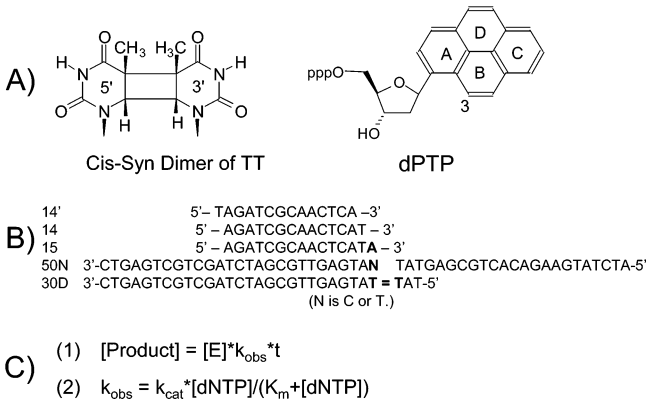

FIGURE 1: DNA substrates and equations used. (A) Structures of the cis-syn dimer of TT and dPTP. (B) DNA primers and templates used in this study. (C) Equations used to fit the kinetic data.

Standing Start Kinetic Experiments. Unless otherwise noted, all reactions were carried out in a reaction buffer containing 40 mM Tris-HCl (pH 7.5), 5 mM $MgCl_2$, 1 mM DTT, 10 μg/mL BSA, and 10% glycerol. Single completed hit standing start steady state single nucleotide insertion reactions were carried out on a large excess of primer−template to pol η at room temperature (temperature controlled at 23 °C) using various concentrations of deoxynucleotide triphosphates in a total volume of 10 μL for the designated time, which was chosen so that less than 20% of the primers were extended. Reactions were initiated by adding pol η and quenched by adding an EDTA solution (final concentration of 100 mM). The quenched reaction mixtures were electrophoresed on a high-resolution denaturing 15% polyacrylamide gel and scanned with a Bio-Rad Phosphorimager. The scanned bands were quantified by the volume integration methods using Quantity One software (Bio-Rad).

Running Start Kinetic Experiments. Single completed hit running start experiments were initiated by mixing 5 μL of a dTTP/dNTP/trap DNA solution (100 μM dTTP, 0−1000 μM dNTP, and 20 μM unlabeled primer/template) with 5 μL of a labeled primer−template/polymerase solution. After 15 s at room temperature, reactions were quenched by adding an EDTA solution (final concentration of 100 mM). The quenched reaction mixtures were electrophoresed on a high-resolution denaturing 15% polyacrylamide gel and imaged with a Bio-Rad Phosphorimager. The scanned bands were quantified by volume integration methods using Quantity One (Bio-Rad).

Simulating and Fitting the Kinetic Data. To determine Michaelis−Menten parameters k_{cat} and K_m from the standing start single nucleotide insertion experiments, the initial insertion rates (k_{obs}) were plotted as a function of nucleotide concentration ([dNTP]) and fit to the Michaelis−Menten equation [$k_{obs} = k_{cat}$[dNTP]/(K_m + [dNTP])]. The running start experiments were analyzed in a similar way except that $(I_2/I_1)_{obs}$, where I_2 equals the sum of the volume integral of the +2 and greater bands and I_1 equals the volume integral

[1] Abbreviations: pol η, polymerase η; dITP, inosine deoxyribose triphosphate; d2APTP, 2-aminopurine deoxyribose triphosphate; dDAPTP, 2,6-diaminopurine deoxyribose triphosphate; d6CPTP, 6-chloropurine deoxyribose triphosphate; d7DATP, 7-deazaadenine deoxyribose triphosphate.

Table 1: Steady State Kinetic Parameters for Insertion of Purine Deoxyribose Monophosphate Derivatives Opposite C or T by Yeast Pol η

template	dNTP	$k_{cat} \pm$ SD (s^{-1})	$K_m \pm$ SD (μM)	k_{cat}/K_m ($s^{-1}\,\mu M^{-1}$)	relative efficiency	WC stability[a]	wobble stability[a]
50-C	P	0.61 ± 0.04	0.94 ± 0.23	0.65	3.8	na	na
	G	1.1 ± 0.02	6.2 ± 0.4	0.17	1.0	3	0/0
	I	0.65 ± 0.01	17 ± 2	0.038	0.22	2	−1/0
	DAP	0.030 ± 0.001	150 ± 20	0.00020	0.0012	−1	2/0
	A	0.015 ± 0.001	73 ± 6	0.00021	0.0012	−2	1/0
	2AP	0.026 ± 0.001	190 ± 30	0.00014	0.00080	0	2/−1
	6CP	0.014 ± 0.001	330 ± 40	0.000043	0.00025	−1	1/−1
50-T	P	0.33 ± 0.02	0.58 ± 0.13	0.57	12	na	na
	A	0.36 ± 0.01	7.5 ± 0.7	0.048	1.0	2	−1/−2
	DAP	0.62 ± 0.02	17 ± 2	0.037	0.77	3	−2/−2
	2AP	1.1 ± 0.09	130 ± 30	0.0084	0.18	2	−2/−1
	6CP	0.43 ± 0.01	320 ± 30	0.0013	0.028	1	−1/−1
	G	0.083 ± 0.003	370 ± 40	0.00022	0.0047	−1	0/2
	I	0.047 ± 0.003	260 ± 50	0.00018	0.0038	−2	1/2

[a] Calculated as the number of donor−acceptor pairs minus the number of donor−donor and acceptor−acceptor pairs. For wobble base pairs, the first term is for the geometry in Figure 3G and the second for that in Figure 3H.

Table 2: Steady State Kinetic Parameters for Insertion of Purine Deoxyribose Monophosphate Derivatives Opposite the 3′- or 5′-T of a Thymine Dimer by Yeast Pol η

template base	dNTP	$k_{cat} \pm$ SD (s^{-1})	$K_m \pm$ SD (μM)	k_{cat}/K_m ($s^{-1}\,\mu M^{-1}$)	relative efficiency	WC stability[a]	wobble stability[a]
3′-T	P	0.49 ± 0.01	0.90 ± 0.09	0.54	76	na	na
	DAP	0.58 ± 0.06	65 ± 2	0.0089	1.3	3	−2/−2
	A	0.24 ± 0.01	34 ± 3	0.0071	1	2	−1/−2
	2AP	0.53 ± 0.03	220 ± 20	0.0024	0.34	2	−2/−1
	6CP	0.064 ± 0.001	460 ± 20	0.00014	0.020	1	−1/−1
	G	0.030 ± 0.001	490 ± 30	0.000061	0.0085	−1	0/2
	I	0.010 ± 0.0006	400 ± 70	0.000025	0.0035	−2	1/2
5′-T	P	0.00055 ± 0.00002	1.1 ± 0.2	0.00050	0.026	na	na
	DAP	0.64 ± 0.01	24 ± 1	0.027	1.4	3	−2/−2
	A	0.53 ± 0.01	28 ± 1	0.019	1	2	−1/−2
	2AP	0.65 ± 0.01	77 ± 3	0.0084	0.44	2	−2/−1
	6CP	0.15 ± 0.002	300 ± 10	0.00050	0.026	1	−1/−1
	I	0.0081 ± 0.0004	230 ± 40	0.000035	0.0018	−2	1/2
	G	0.0063 ± 0.0001	410 ± 20	0.000015	0.00079	−1	0/2

[a] Calculated as the number of donor−acceptor pairs minus the number of donor−donor and acceptor−acceptor pairs. For wobble base pairs, the first term is for the geometry in Figure 3G and the second for that in Figure 3H.

Table 3: Steady State Kinetic Parameters for Insertion of Adenosine Monophosphate and Analogues Opposite T and the 3′- or 5′-T of a Thymine Dimer by Yeast Pol η[a]

template base	dNTP	$k_{cat} \pm$ SD (s^{-1})	$K_m \pm$ SD (μM)	k_{cat}/K_m ($s^{-1}\,\mu M^{-1}$)	relative efficiency	WC stability[b]	Hoogsteen stability[b]
T	DAP	0.59 ± 0.01	9.4 ± 0.7	0.063	0.79	3	2
	A	0.31 ± 0.01	3.9 ± 0.9	0.080	1	2	2
	2AP	0.94 ± 0.04	190 ± 20	0.0049	0.061	2	1
	7DA	0.18 ± 0.01	2.7 ± 0.9	0.066	0.83	2	0
3′-T of dimer	DAP	0.59 ± 0.01	19 ± 1	0.031	2.3	3	2
	A	0.31 ± 0.01	23 ± 2	0.014	1	2	2
	2AP	0.79 ± 0.05	200 ± 30	0.0039	0.28	2	1
	7DA	0.25 ± 0.01	15 ± 2	0.017	1.2	2	0
5′-T of dimer	DAP	0.94 ± 0.03	20 ± 2	0.047	1.2	3	2
	A	0.89 ± 0.03	23 ± 3	0.039	1	2	2
	2AP	1.03 ± 0.05	170 ± 20	0.0063	0.16	2	1
	7DA	0.81 ± 0.02	17 ± 1	0.049	1.3	2	0

[a] Carried out with a preparation of enzyme different from that used in Tables 1 and 2. [b] Calculated as the number of donor−acceptor pairs minus the number of donor−donor and acceptor−acceptor pairs.

of the +1 band, was plotted against the dNTP concentration and fit to the equation $(I_2/I_1)_{obs} = (I_2/I_1)_{max}[dNTP]/(K_m + [dNTP])$ as previously described (*22*). All data were fit by nonlinear regression analysis with Scientist version 2.01.

RESULTS

Our goal was to determine the role of H-bonding and base pair geometry in the selection of nucleotides for insertion opposite C, T, and the 3′- and 5′−Ts of the cis-syn thymine dimer by yeast DNA polymerase η (pol η). To do so, we examined the insertion efficiency of various base-modified nucleotides that would be capable of base pairing with pyrimidines in either Watson−Crick, wobble, or Hoogsteen geometries with varying numbers of H-bonds as shown in Figures 3, 5, and 7. The relative stabilities of the base pairs are given in Tables 1−3, and were arbitrarily calculated as the number of donor−acceptor pairs minus the number of donor−donor or acceptor−acceptor pairs. Donor−donor pairs are expected to be unfavorable because they result in bad steric and electrostatic interactions that would have to be compensated by movement of the bases which could in turn cause bad steric interactions with the enzyme active site.

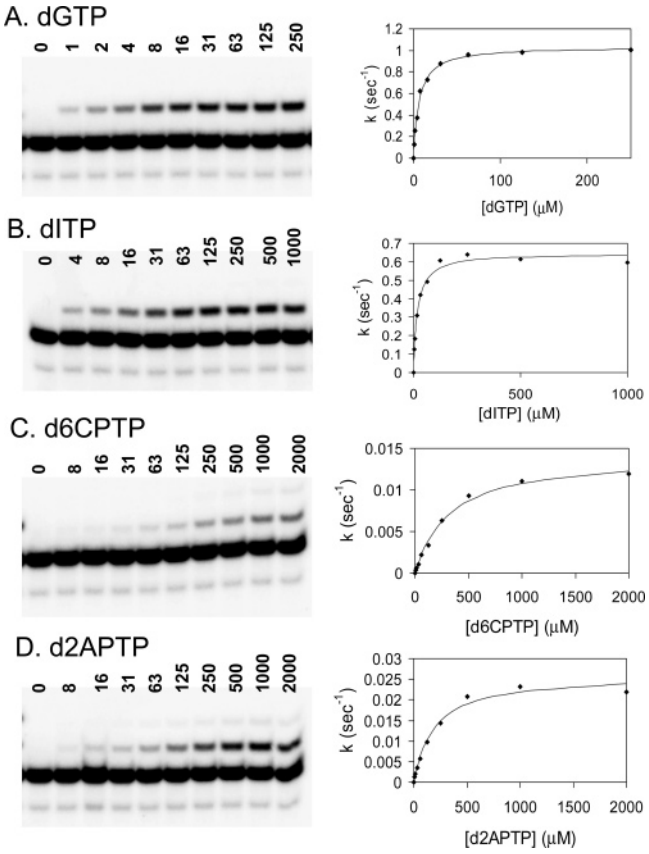

FIGURE 2: Steady state kinetics of nucleotide insertion opposite a C by yeast pol η. The rate of nucleotide insertion was plotted as a function of nucleotide concentration for (A) dGTP, (B) dITP, (C) d6CPTP, and (D) d2APTP. The solid line represents the best fit to the Michaelis−Menten equation, and the k_{cat} and K_m values are listed in Table 1 along with those for dATP and dDAPTP.

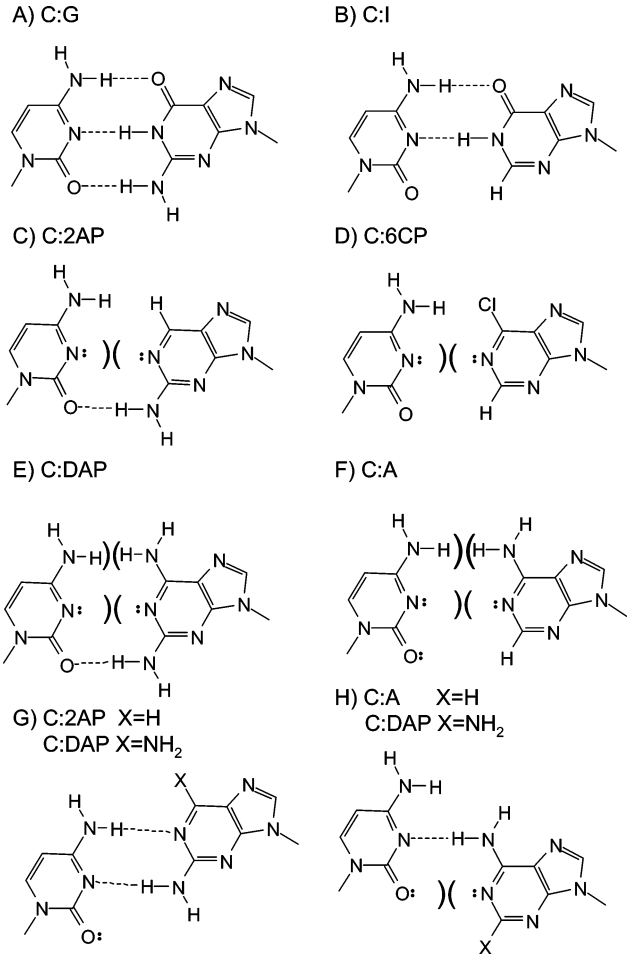

FIGURE 3: Watson−Crick (A−F) and wobble (G and H) base pairing with C. A is adenine, C cytosine, G guanine, T thymine, 6CP 6-chloropurine, I inosine, 2AP 2-aminopurine, and DAP 2,6-diaminopurine. Repulsive steric and electrostatic interactions are indicated with a pair of inverted parentheses.

Acceptor−acceptor pairs do not cause any steric interactions, but have an unfavorable electrostatic interaction. The two types of wobble base pair geometries are illustrated by the structures shown in panels G and H of Figures 3 and 5.

Insertion of Base-Modified Nucleotides Opposite C and T. The efficiencies (k_{cat}/K_m in μM^{-1} s^{-1}) (Table 1) of nucleotide insertion opposite cytosine (Figure 2) appear to correlate best with a complementary Watson−Crick base pair geometry (Figure 3), with a value of 0.17 for G (three H-bonds) and an approximately 4-fold lower value of 0.038 for I (two H-bonds). Both of these nucleotides were inserted with high k_{cat} values of ~1 s^{-1} and low K_m values of ~12 μM. In comparison, there is an approximately 640-fold drop in efficiency for DAP, A, 2AP, and 6CP, which can make at most one H-bond in a Watson−Crick geometry, but because of unfavorable donor−donor and acceptor−acceptor interactions are expected to have much lower stabilities. Most of the drop in efficiency of these latter nucleotides is due to an ≈40-fold decrease in k_{cat} coupled with an ≈16-fold increase in K_m. Arguing against wobble base pairing of the type shown in Figure 3G is the fact that DAP and 2AP are inefficiently inserted even though they could make two H-bonds each without any bad interactions.

The insertion efficiencies of nucleotides opposite thymine (Table 1 and Figure 4) also correlate best with a complementary Watson−Crick base pair geometry (Figure 5) as the highest efficiencies of 0.048 and 0.037 were observed for A and DAP which could make two and three H-bonds, respectively. Both of these nucleotides were inserted with high k_{cat} values of ~0.5 s^{-1} and low K_m values of ~12 μM. There was an approximately 5-fold drop in efficiency on going to 2AP and another 6-fold drop on going to 6CP which would make two H-bonds and one H-bond, respectively, in a Watson−Crick geometry. While the k_{cat} values for insertion of these nucleotides are actually slightly higher than those for A and DAP, the K_m values are approximately 20-fold higher. The efficiency drops an additional 17-fold on going to G and I which make one and no H-bonds, respectively, and both of which have unfavorable donor−donor and acceptor−acceptor interactions (Figure 5). Wobble base pairing of the type shown in Figure 5G is likewise ruled out by the fact that G and I are very inefficiently inserted even though they would have be expected to make two H-bonds without any unfavorable interactions.

Insertion of Base-Modified Nucleotides Opposite the 3′- and 5′-Ts of the Cis-Syn Thymine Dimer. The nucleotide insertion efficiencies opposite the 3′- and 5′-Ts of the cis-syn thymine dimer were expected to be qualitatively the same as for a normal T because the H-bonding pattern of both Ts is retained, although the 5′-T of the dimer appears to be out of plane in a crystal structure of a dimer-containing duplex, and not able to make good H-bonds (*23*). The insertion

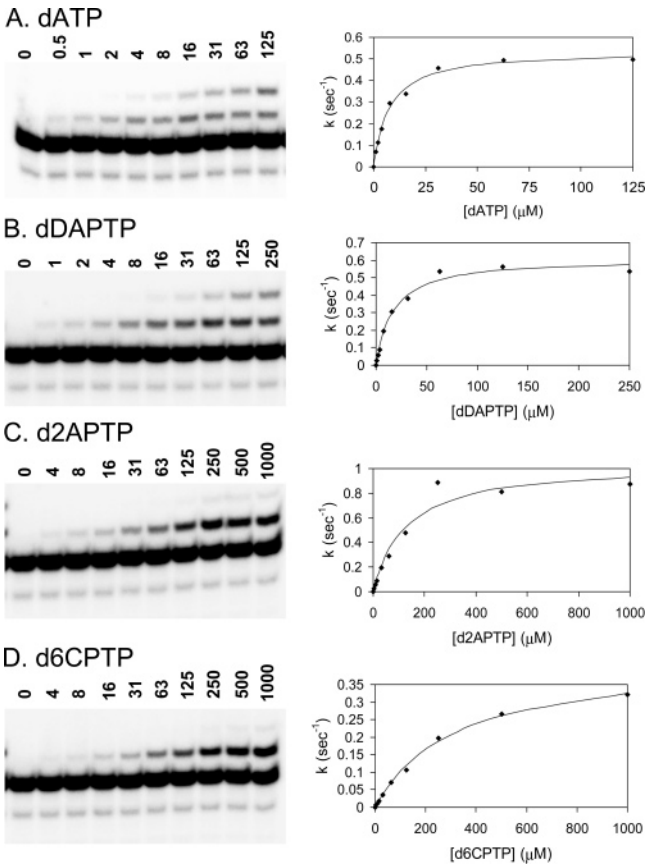

FIGURE 4: Steady state kinetics of nucleotide insertion opposite a T by yeast pol η. The rate of nucleotide insertion was plotted as a function of each nucleotide concentration for (A) dATP, (B) dDAPTP, (C) d2APTP, and (D) d6CPTP. The solid line represents the best fit to the Michaelis−Menten equation, and the k_{cat} and K_m values are listed in Table 1 along with data for dGTP and dITP.

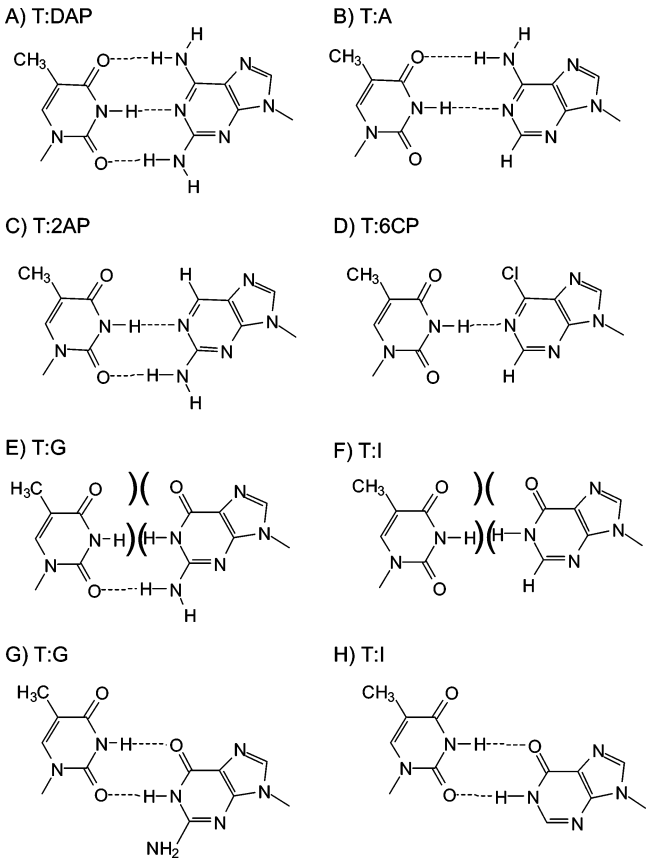

FIGURE 5: Watson−Crick (A−F) and wobble (G and H) base pairing with T. A is adenine, C cytosine, G guanine, T thymine, 6CP 6-chloropurine, I inosine, 2AP 2-aminopurine, and DAP 2,6-diaminopurine. Repulsive steric and electrostatic interactions are indicated with a pair of inverted parentheses. The same base pairings would apply to the 3′-T and 5′-T of a thymine dimer.

efficiencies (k_{cat}/K_m in μM^{-1} s^{-1}) opposite the 3′-T of the dimer (Table 2) are consistent with the involvement of Watson−Crick base pairing with values of 0.0089, 0.0071, and 0.0024 for DAP, A, and 2AP, respectively, which make from two to three H-bonds (Figure 5). This is followed by an approximately 90-fold drop in efficiency on going to 6CP, G, and I which make from zero to one H-bond in a Watson−Crick geometry (Figure 5). The large drop in efficiency is due to an ≈13-fold drop in k_{cat} and an ≈4-fold increase in K_m. The results for insertion of nucleotides opposite the 5′-T of the dimer are quite similar to those for the 3′-T, except that the insertion efficiencies of G and I are ∼20-fold lower than for 6CP, compared to only ∼3-fold lower in the case of the 3′-T (Table 2). The large drop in efficiencies for insertion of G and I opposite the 5′-T compared to that for 6CP can be attributed to an increase in the efficiency for insertion of 6CP and a decrease in the efficiencies for insertion of G and I (Figure 6).

To determine whether insertion of A opposite the 5′- and 3′-Ts of the dimer is occurring by Watson−Crick or Hoogsteen base pairing, 7DA (7-deazaadenine) insertion was also compared with A, 2AP, and DAP, and found to be inserted with slightly higher efficiency than A (Figure 6 and Table 3). Had Hoogsteen base pairing been involved, 7DA would have been expected to be much less efficiently inserted due to an unfavorable steric interaction between the proton on N7 of 7DA and the N3-NH group of T (Figure 7).

Nucleotide Insertion by Exo⁻ Klenow Fragment. To determine the extent to which nucleotide selection by pol η differs from that of replicative polymerases, we examined the selectivity of nucleotide analogue insertion by the Klenow fragment. Experiments conducted under single completed hit steady state standing start conditions used in our pol η studies and commonly used by many others for a variety of polymerases led to the unexpected result that 2-aminopurine (2AP) insertion opposite T by the Klenow fragment was 12 times more efficient than that of A, and that 6-chloropurine (6CP) was 2 times more efficient than A as calculated from the ratio of their apparent k_{cat}/K_m values (data not shown). It was expected, however, that the efficiency of 2-aminopurine insertion opposite T would have been ∼20% of that of A insertion based on a careful study using both pre-steady state and running start experiments, as well as direct competition experiments (*22*). The discrepancy can be attributed to the fact that the rate-limiting step in nucleotide insertion of dAMP opposite T by the Klenow fragment is product release (k_{off}) rather than nucleotide insertion (k_{pol}) [0.06 and 50 s^{-1}, respectively (*24*)], and that products terminating in 2-aminopurine opposite a T are released much more rapidly than those terminating in an A. Thus, in the absence of a polymerase trap to prevent reassociation, the polymerase will turn over more rapidly following insertion of 2-aminopurine nucleotide than following insertion of A, giving the appearance that 2-aminopurine insertion is more efficient.

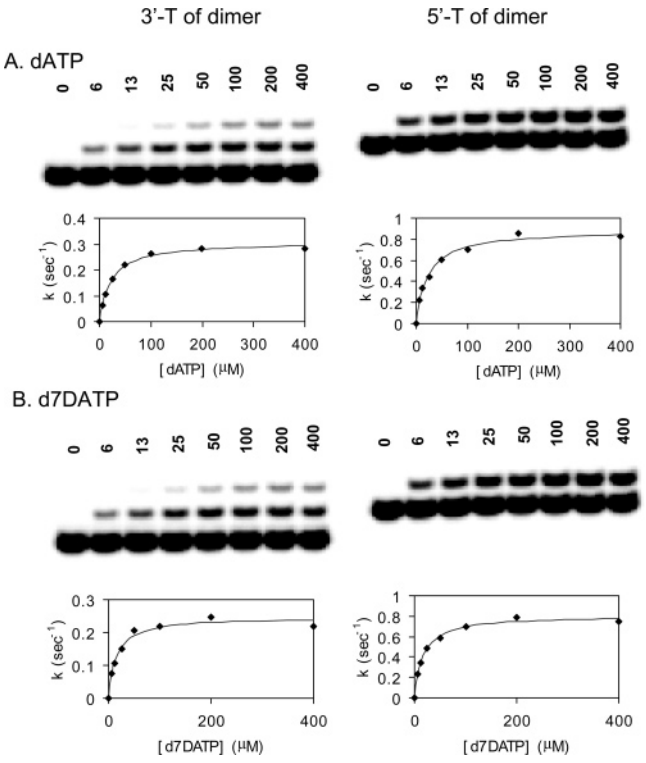

FIGURE 6: Steady state kinetics of insertion opposite the 3′-T and 5′-T of the cis-syn thymine dimer with dATP and d7DATP by yeast pol η. The rate of nucleotide insertion was plotted as a function of nucleotide concentration. The solid line represents the best fit to the Michaelis−Menten equation, and the k_{cat} and K_m values are listed in Table 3 together with those for dDAPTP and d2APTP.

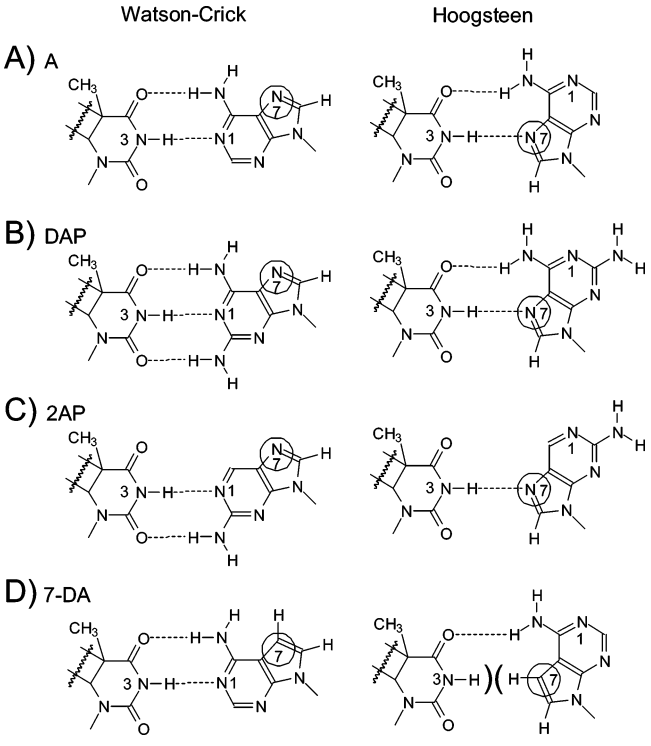

FIGURE 7: Watson−Crick and Hoogsteen base pairings with the 3′-T or 5′-T of the cis-syn thymine dimer. A is adenine, DAP 2,6-diaminopurine, 2AP 2-aminopurine, and 7DA 7-deazaadenine. Repulsive steric and electrostatic interactions are indicated with a pair of inverted parentheses, and the N7 position is circled.

To eliminate contributions to the observed insertion rate from k_{off}, we carried out the insertion experiments under single completed hit running start conditions as previously described (*22*). Under these experimental conditions, the polymerase must first add one or more nucleotides before reaching the target template nucleotide at which point it can either dissociate or insert a nucleotide. When the experiments were carried out under single hit conditions by either using excess template primer or in the presence of excess cold primer−template as a trap, the observed sum of the integrated intensity of all bands terminating opposite and following the target (I_i) divided by the integrated intensity of the band terminating prior to the target site (I_{i-1}) is equal to k_{ins}/k_{off}. A plot of $(I_i/I_{i-1})_{obs}$ versus dNTP concentration follows Michaelis−Menten kinetics and can be fit to the relation $(I_i/I_{i-1})_{obs} = (I_i/I_{i-1})_{max}[dNTP]/([dNTP] + K_m)$, where $(I_i/I_{i-1})_{max} = k_{pol}/k_{off}$. Since k_{off} is independent of the nucleotide being inserted opposite the target, the relative selectivity for insertion of two nucleotides is equal to the ratio of their $(I_i/I_{i-1})_{max}/K_m$ values.

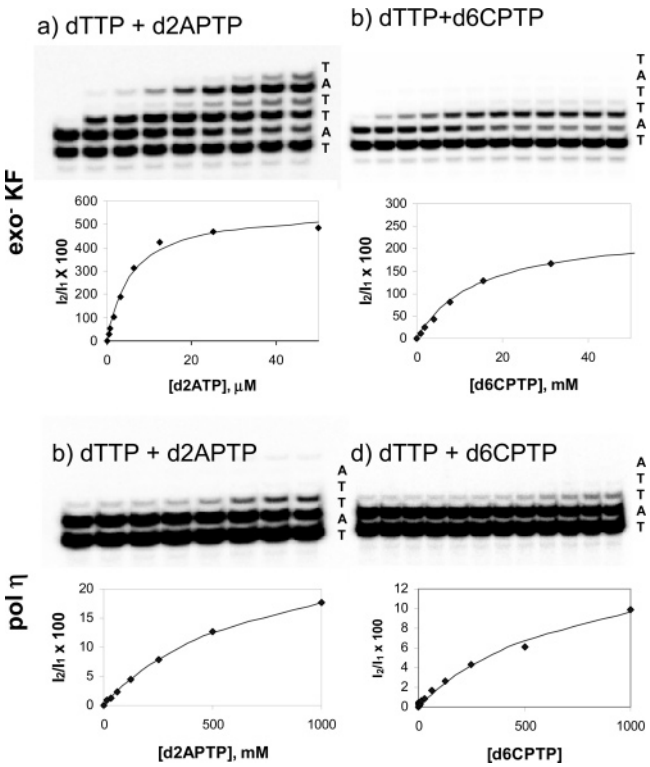

FIGURE 8: Running start single completed hit experiments of nucleotide insertion opposite the T with d2APTP and d6CPTP by exo⁻ Klenow fragment and yeast pol η. The 14′ primer−template (100 nM) was preequilibrated with 100 units/mL exo⁻ Klenow fragment or 100 nM pol η, and then 100 μM dTTP and various concentrations of d2APTP or d6CPTP were added together with 20 μM 26-mer/50T primer−template as a trap for 15 s. The I_2/I_1 ratio, which equals the sum of the volume integrals for all +2 and greater bands (I_2) to that of the +1 band (I_1), was plotted as a function of the nucleotide concentration. The solid line represents the best fit to the Michaelis−Menten equation, and the I_2/I_1 and K_m values are listed in Table 4 together with those for the other nucleotide triphosphates. Concentrations of dNTP from left to right were (a) 0, 0.4, 0.8, 1.6, 3.1, 6.3, 13, 25, and 50 μM, (b) 0, 1, 2, 4, 8, 16, 31, 63, 125, 250, 500, and 1000 μM, (c) 0, 16, 32, 63, 125, 250, 500, and 1000 μM, and (d) 0, 1, 2, 4, 8, 16, 32, 63, 125, 250, 500, and 1000 μM.

In our experiments (Figure 8), a 14-mer primer terminating two nucleotides before the target T or C (14′) was incubated with a constant concentration of dTTP (the next correct base) and varying concentrations of the nucleotide of interest in

Table 4: Relative Efficiency of Nucleotide Insertion Opposite T and C by Exo$^-$ Klenow Fragment and Yeast Pol η Carried Out under Running Start Single Completed Hit Conditions

pol	template base	dNTP	$(I_2/I_1)_{max} \pm$ SD ($\times$100)	$K_m \pm$ SD (μM)	$(I_2/I_1)_{max}/K_m$ ($\times$ 100)	relative efficiency
exo$^-$ KF	T	A	650 ± 4	0.34 ± 0.01	1900	1
		DAP	610 ± 10	0.36 ± 0.4	1700	0.89
		2AP	570 ± 20	5.6 ± 0.7	100	0.053
		CP	240 ± 4	15 ± 1	16	0.0084
		G	2.9 ± 0.1	80 ± 12	0.036	0.000019
	C	G	570 ± 8	0.53 ± 0.04	1100	1
		I	480 ± 8	6.2 ± 0.3	77	0.072
		A	8.3 ± 0.5	180 ± 24	0.046	0.000043
pol η	T	A	110 ± 1	250 ± 9	0.44	1
		DAP	108 ± 2	250 ± 10	0.43	0.98
		2AP	30 ± 0.6	720 ± 30	0.042	0.095
		CP	17 ± 2	760 ± 140	0.022	0.051
		G	4.4 ± 0.2	990 ± 100	0.0044	0.01
	C	G	360 ± 20	200 ± 30	1.8	1
		I	160 ± 4	400 ± 20	0.39	0.22
		A	4.4 ± 0.4	590 ± 150	0.0075	0.0042

the presence of a large excess of unlabeled template−primer as a DNA polymerase trap to prevent turnover. The values of $(I_2/I_1)_{max}$ and K_m that we obtained from fitting the $(I_2/I_1)_{obs}$ data are listed in Table 4. Under these conditions, we found that the selectivity of 2-aminopurine insertion by Klenow fragment was 5% of that of A which is close to the value of 20% previously reported in another sequence context (*22*). The relative misinsertion efficiencies of 1.9×10^{-5} for G opposite T and 4.3×10^{-5} for A opposite C are also similar to reported values of 7.1×10^{-5} and 5.3×10^{-5} from mutagenesis studies (*25*).

We have previously found that nucleotide insertion selectivities for the catalytic core of yeast pol η obtained from standing start experiments are very similar to those obtained from pre-steady state experiments and direct competition experiments, indicating that the reaction efficiencies under steady state conditions are largely determined by k_{pol} and not by k_{off} (*26*). To be sure, however, we also repeated the nucleotide insertion selectivity experiments for pol η under the same running start conditions used for the Klenow fragment and obtained selectivities (Table 4) similar to those obtained under the standing start conditions (Tables 1 and 3). The relative misinsertion efficiencies of 0.010 for G opposite T and 0.0042 for A opposite C obtained under the running start conditions are similar to those of 0.0047 and 0.0012 obtained under standing start conditions by us (Table 1) and the previously reported values of 0.0053 and 0.0058, also obtained under standing start conditions (*27*). We did find, however, that the apparent K_m values obtained from the running start experiments were much higher than that obtained under pre-steady state or standing start conditions which we attribute to competitive inhibition by the 100 μM dTTP. Indeed, when lower concentrations of dTTP were used, the apparent K_m values were reduced (data not shown).

DISCUSSION

Polymerase η, encoded by the Rad30A gene, is one of the newly discovered DNA damage bypass polymerases of the UmuC/DinB/Rev1/RAD30 superfamily, or Y-family polymerases (*28*−*33*). Pol η has been of great interest because of its ability to bypass the cis-syn thymine dimer efficiently and relatively nonmutagenically (*34*, *35*), and because defects in the human enzyme have been linked to the genetic disease xeroderma pigmentosum (*36*−*38*). Unlike replicative polymerases which are capable of high-fidelity synthesis, the DNA damage bypass polymerases typified by pol η are much more error prone (*27*, *29*, *39*−*41*). The lower fidelity of the DNA damage bypass polymerases has been attributed to their much more open and less constrained active site that enables them to bypass DNA damage and their ability to better tolerate mismatched DNA than the more constrained replicative polymerases. Because of the less constrained active site of Y-family polymerases as gleaned from X-ray crystal structures of Dpo4 (*16*, *42*) and pol η (*43*), complementary nucleotide selection may depend more on base stacking and base pairing than on steric fit as has been found for the Klenow fragment of *E. coli* DNA polymerase I and some other polymerases (*44*, *45*).

Evidence that base pairing and stacking play an important role in nucleotide selection by yeast pol η comes from recent experiments with the non-hydrogen bonding thymine analogue, difluorotoluene nucleotide (dFTP), and the nonpolar base pair mimic, pyrene nucleotide (dPTP). Although difluorotoluene cannot form hydrogen bonds with A, the Klenow fragment inserts difluorotoluene nucleotide opposite A only 40-fold less efficiently than T, whereas yeast pol η inserts difluorotoluene nucleotide 220-fold less efficiently (*15*). These data suggest that Klenow fragment selects nucleotides primarily by their ability to adopt a Watson−Crick base pair shape [the steric exclusion model (*8*−*10*)], whereas pol η appears to require other and/or additional interactions for efficient nucleotide insertion, such as complementary H-bonding. In accord with the steric exclusion model, Klenow fragment is unable to efficiently insert pyrene nucleotide opposite a normal template base because it cannot fit (*11*). On the other hand yeast pol η can efficiently insert pyrene nucleotide opposite a normal base, presumably because of its superior base pair stacking ability and its ability to trigger the conformational change that precedes phosphodiester bond formation (*12*). In this paper, we have investigated further the importance of H-bonding and base pair geometry for nucleotide selection by pol η by examining the insertion efficiency of a series of purine analogues opposite C and T, and both Ts of a thymine dimer.

Watson−Crick H-Bonding between the Template Base and the Incoming Nucleotide Is Required for the Accurate and

Efficient DNA Synthesis by Pol η. We examined the insertion efficiencies of commercially available purine deoxynucleotide triphosphate analogues guanine (dGTP), adenine (dATP), 6-chloropurine (d6CPTP), inosine (dITP), 2-aminopurine (d2APTP), and 2,6-diaminopurine (dDAPTP). These nucleotides are capable of forming up to three H-bonds with cytosine or thymine in Watson−Crick, wobble, and Hoogsteen base pair geometries. The insertion efficiencies were found to parallel the ability to form Watson−Crick base pairs and not wobble or Hoogsteen bases pairs. Insertion opposite cytosine was the most efficient for dGTP, which can form three H-bonds with C, whereas dITP, which lacks the N2 amino group and can only form two H-bonds with C, was inserted 5-fold less efficiently. Both dGTP and dITP were much more efficiently inserted than dATP and other analogues which could have made up to two H-bonds in Wobble base pair geometries.

Insertion opposite thymine is likewise most efficient with nucleotides capable of Watson−Crick base pairing, though they did not correlate as directly with the total number of H-bonds. Thus, A, which can form two H-bonds, is inserted with approximately the same efficiency as diaminopurine (DAP), which can form three H-bonds, and ~10-fold more efficiently than 2AP, which can also form two H-bonds (Tables 1, 3, and 4). Unlike the case of inosine, in which replacing H2 with an amino group to give G results in a large increase in insertion efficiency opposite C, replacing H2 of adenine with an amino group to give DAP appears to have no significant effect on insertion efficiency opposite T despite adding another H-bond. The difference cannot be due to a steric effect, as adding an amino group to the 2-position of adenine should not be any different than adding an amino group to the 2-position of inosine. The 2-amino group might, however, influence the electronics of the purine ring of adenine and inosine differently, which could result in differences in base stacking affinity or base stacking geometry that offset any gain in H-bonding. In support of this idea, the thermostability of a DAP:T base pair-containing duplex has been reported to be lower than that of the corresponding G·C base pair-containing duplex, although both pairs form three H-bonds (*46*−*48*). The stability of a DAP·T base pair has also been found to depend on flanking sequence, and this base pair is 0.9 kcal/mol less stable than the corresponding A·T base pair in the sequence d(CA_3XA_3G)·(CT_3YT_3G), but more stable by 0.3 kcal/mol when the base pair is inverted (*49*). When flanked by G·C base pairs in d(C_3XG_3)·d(C_3YG_3), the DAP·T base pair is more stable than the A·T base pair by 0.9 kcal/mol.

In accord with the idea that replacing H2 of A with an amino group does not affect the insertion efficiency opposite T, moving the amino group from the 6-position of A to the 2-position causes an ~10-fold decrease in insertion efficiency (Tables 1, 3, and 4) that can be attributed to loss of the H-bond with the 6-amino group. The decrease in efficiency can be attributed to a 17-fold increase in K_m from ~6 μM for A to 160 μM for 2AP, which is offset by an approximately 3-fold increase in k_{cat} (Tables 1 and 3). A 5-fold decrease in efficiency has also been reported for insertion of 2AP by exo$^-$ Klenow fragment which could be almost exclusively attributed to an increase in K_m (*22*). For our template, the efficiency of 2AP insertion opposite T by exo$^-$ KF is almost 20-fold lower and can likewise be attributed almost exclusively to K_m. The increase in K_m is consistent with thermodynamic studies of d(CGTACXCATGC)·d(GCATGTGTACG) which found that the duplex is ~0.5 kcal/mol less stable when X is 2AP than when it is A (*3*).

Additional evidence for the important contribution that H-bonding can make to insertion efficiency for pol η comes from comparing the efficiency of 6-chloropurine nucleotide insertion opposite C and T (Table 1). Whereas insertion opposite C occurs with an efficiency of 0.00025 s^{-1} μM^{-1}, insertion opposite T occurs with a more than 100-fold higher efficiency. This can be explained by the inability of 6CP to form H-bonds with C in a Watson−Crick geometry coupled with the presence of an unfavorable acceptor−acceptor interaction, compared to the single H-bond that can be formed between T and 6CP, and the absence of any unfavorable interactions. The behavior of 6CP nucleotide toward insertion opposite C is similar to that observed for insertion of difluorotoluene (F) nucleotide opposite A (*15*), except that it is almost 20 times less efficient. The lower efficiency of inserting 6CP opposite C compared to inserting F opposite A may be due to the additional presence of an unfavorable acceptor−acceptor interaction between 6CP and C that is not present between F and A.

Comparison to Klenow Fragment. Interestingly, the relative selectivities for inserting A, DAP, 2AP, and 6CP opposite T and G and I opposite C by exo$^-$ Klenow fragment are very similar to those observed for pol η (Table 4). This similarity would suggest that nascent base pairs having the same Watson−Crick geometry can be further discriminated on the basis of a common set of H-bonding and base stacking interactions. It has been reported, however, that difluorotoluene nucleotide which cannot make H-bonds was inserted opposite A by the Klenow fragment only 40 times less efficiently than T (*8*), and that A was inserted opposite difluorotoluene only 4 times less efficiently than opposite T (*50*). These results were taken to suggest that H-bonding may not play a very important role in nucleotide selection by the Klenow fragment. It is important to note, however, that these efficiencies were obtained from standing start experiments without a polymerase trap, and may be overestimated due to more rapid turnover of the products containing difluorotoluene. This is entirely possible, as we have found that standing start experiments with the Klenow fragment resulted in 225- and 240-fold overestimations of the 2-aminopurine and 6-chloropurine insertion efficiencies, respectively, opposite T compared to the insertion of A. If so, it may be that the relative insertion efficiencies for difluorotoluene nucleotide or for nucleotides opposite difluorotoluene by the Klenow fragment compared to T are more similar to the approximately 200-fold lower efficiencies observed for pol η (*15*), though this remains to be determined.

The parallel observed in nucleotide insertion efficiencies between the Klenow fragment and pol η for Watson−Crick-like base pairs ends with mismatched base pairs. Whereas the misinsertion efficiencies for yeast pol η are ~0.01 and ~0.004 for inserting G opposite T and A opposite C, respectively, as observed by us (Tables 1 and 4) and by others (*27*), the corresponding misinsertion efficiencies are ~500- and ~100-fold lower, respectively, for the Klenow fragment (Table 4) (*25*). The lower misinsertion efficiencies would be consistent with the greater shape selectivity of the Klenow fragment than pol η. Likewise, the relative misinsertion

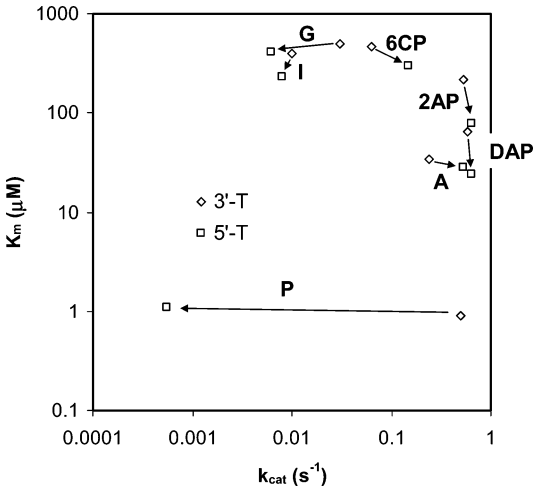

FIGURE 9: Log−log plot of the k_{cat} and K_m values of Table 2 for insertion opposite the 3′- and 5′-Ts of the cis-syn thymine dimer. The arrows point from the kinetic parameters for the 3′-T to those for the 5′-T.

efficiencies of difluorotoluene nucleotide by the Klenow fragment resemble those for natural mispairs ($\approx 10^{-4}$), whereas the relative misinsertion efficiencies for pol η differ by less than 3. The latter result would suggest that without H-bonding to hold a base pair in place, there can be little discrimination between mispairs by pol η in accord with a more open, less constrained active site.

Nucleotide Insertion Opposite the Cis-Syn Thymine Dimer by Pol η Occurs via Watson−Crick and Not Hoogsteen Base Pairing. Recently, a set of crystal structures of Dpo4 from *Sulfolobus solfataricus*, another Y-family polymerase, have been obtained in various stages of synthesis past a cis-syn thymine dimer. What is most notable about these structures is that whereas the 3′-T of the dimer was found to form the expected Watson−Crick base pair with the incoming ddATP, the 5′-T was found to form a Hoogsteen base pair (*51*). Because Dpo4 is also a member of the Y-family polymerases, it is possible that insertion of A opposite a cis-syn dimer by pol η might also occur via a Hoogsteen base pair. We tested this possibility by using 7-deazaadenine (7DA), which is identical to A except that it has a CH group substituted for N7. Whereas A can make two H-bonds with T in both Watson−Crick and Hoogsteen base pair geometries, 7DA can make two H-bonds with T in the Watson−Crick geometry but only one in the Hoogsteen geometry (Figure 7). The Hoogsteen base pair between 7DA and T is also further destabilized by a bad steric interaction between H7 of 7DA and H3 of T (Figure 7). Since the insertion efficiencies for dATP and d7DATP are almost identical, we conclude that insertion of dAMP is most likely occurring via a Watson−Crick geometry.

Insertion Opposite the 5′-T of the Dimer Is More Selective than That Opposite the 3′-T. An interesting feature of dimer bypass is revealed when the relative nucleotide insertion efficiencies opposite the 3′- and 5′-Ts of the dimer are compared (Table 2 and Figure 9). It appears that the insertion efficiencies of nucleotides capable of Watson−Crick base pairing (A, DAP, 2AP, and 6CP) increase opposite the 5′-T compared with the 3′-T, whereas the efficiencies of the nucleotides incapable of Watson−Crick base pairing decrease (G) or remain relatively the same (I). Though a higher selectivity for insertion of A opposite the 5′-T of the dimer than the 3′-T was not observed in an earlier fidelity study of yeast pol η (*34*), it has recently been observed for human pol η (*52*). The higher selectivity observed for insertion opposite the 5′-T is initially surprising given the fact that both solution NMR (*53*−*55*) and crystal structure (*23*) data indicate that the 5′-T of the thymine dimer is not able to base pair as well as the 3′-T due to its distorted nature. Recently, we have obtained evidence that the 5′-T of the dimer is held more tightly during nucleotide insertion than the 3′-T by pol η (*12*), and it is possible that this may help to enforce Watson−Crick base pairing with the 5′-T and thereby compensate for its otherwise poorer base pairing geometry. Holding the 5′-T of the dimer rigidly in a conformation that is favorable for Watson−Crick base pairing could also serve to disfavor base pairing with alternate geometries that would require repositioning of the T.

The proposal that the 5′-T of the dimer must be held much more tightly during insertion opposite it by pol η than the 3′-T when a nucleotide is being inserted opposite it was based on the results of insertion experiments with pyrene nucleotide. It was observed that pyrene nucleotide is inserted with high efficiency and in preference to other nucleotides opposite the 3′-T of the thymine dimer, but with extremely low efficiency opposite the 5′-T of the dimer (*12*). Because of its size, pyrene nucleotide cannot be inserted without first displacing the templating nucleotide and, in the case of the Klenow fragment or T7 polymerase, cannot be inserted opposite normal nucleotides (*11*). Pyrene can be inserted, however, by the Klenow fragment or T7 polymerase opposite an abasic site because there is no templating base present (*11*), or opposite the 3′-T of a dinucleotide photoproduct because the dimer is so large that it cannot enter the active site and thus behaves like an abasic site (*56*). In contrast to these pol A family polymerases, pol η inserts pyrene nucleotide in preference to the complementary nucleotide opposite most templating nucleotides, indicating that pol η does not hold on tightly to the templating nucleotide (*12*). Because the 3′-T is covalently fused to the 5′-T of the dimer, however, the ability of the 3′-T or the 5′-T to be displaced depends on how tightly either or both the 3′-T and the 5′-T of the dimer are being held by the polymerase. The ability to efficiently insert pyrene nucleotide opposite the 3′-T of the dimer indicates that neither the 3′-T nor the 5′-T of the dimer must be held tightly when the 3′-T is in the templating site and thus can be displaced by pyrene. Pyrene nucleotide cannot be inserted opposite the 5′-T of the dimer, however, which can only be explained if pol η is holding on tightly to the 3′-T of the dimer when the 5′-T is in the templating site, thereby preventing the 5′-T from being displaced. This makes sense because during insertion opposite the 5′-T of the dimer, the 3′-T is positioned within the duplex DNA binding domain of the polymerase.

CONCLUSION

It appears that pol η selects nucleotides for insertion opposite pyrimidines and thymine dimers on the basis of a combination of H-bonding and base stacking in a Watson−Crick geometry, and not Hoogsteen or wobble geometries. It also appears that the nucleotide insertion selectivity of pol η parallels that of the Klenow fragment for Watson−Crick-like base pairs, but not for mismatches, emphasizing the

importance of H-bonding in nucleotide selection by both polymerases, but lesser shape selection by pol η due to its more open and relaxed active site. More studies will be needed, however, to dissect the energetics of nucleotide binding and insertion by pol η in comparison to the A-family polymerases.

ACKNOWLEDGMENT

We thank Hussam Bdour for the dimer-containing oligodeoxynucleotide, Liping Sun for pyrene nucleotide, and Vincent Cannistraro for help with some of the experiments.

REFERENCES

1. Aboul-ela, F., Koh, D., Tinoco, I., Jr., and Martin, F. H. (1985) Base−base mismatches. Thermodynamics of double helix formation for dCA3XA3G + dCT3YT3G (X, Y = A, C, G, T), *Nucleic Acids Res. 13*, 4811−4824.
2. Petruska, J., Goodman, M. F., Boosalis, M. S., Sowers, L. C., Cheong, C., and Tinoco, I., Jr. (1988) Comparison between DNA melting thermodynamics and DNA polymerase fidelity, *Proc. Natl. Acad. Sci. U.S.A. 85*, 6252−6256.
3. Law, S. M., Eritja, R., Goodman, M. F., and Breslauer, K. J. (1996) Spectroscopic and calorimetric characterizations of DNA duplexes containing 2-aminopurine, *Biochemistry 35*, 12329−12337.
4. Kunkel, T. A., and Bebenek, K. (2000) DNA replication fidelity, *Annu. Rev. Biochem. 69*, 497−529.
5. Sloane, D. L., Goodman, M. F., and Echols, H. (1988) The fidelity of base selection by the polymerase subunit of DNA polymerase III holoenzyme, *Nucleic Acids Res. 16*, 6465−6475.
6. Goodman, M. F. (1997) Hydrogen bonding revisted: Geometric selection as a principal determinant of DNA replication fidelity, *Proc. Natl. Acad. Sci. U.S.A. 94*, 10493−10495.
7. Showalter, A. K., and Tsai, M. D. (2002) A reexamination of the nucleotide incorporation fidelity of DNA polymerases, *Biochemistry 41*, 10571−10576.
8. Moran, S., Ren, R. X.-F., and Kool, E. T. (1997) A thymidine triphosphate shape analog lacking Watson−Crick pairing ability is replicated with high sequence selectivity, *Proc. Natl. Acad. Sci. U.S.A. 94*, 10506−10511.
9. Moran, S., Ren, R. X.-F., Rumney, S. I. V., and Kool, E. T. (1997) Difluorotoluene, a nonpolar isostere of thymine, codes specifically and efficiently for adenine in DNA replication, *J. Am. Chem. Soc. 119*, 2056−2057.
10. Kool, E. T. (1998) Replication of non-hydrogen bonded bases by DNA polymerases: A mechanism for steric matching, *Biopolymers 48*, 3−17.
11. Matray, T. J., and Kool, E. T. (1999) A specific partner for abasic damage in DNA, *Nature 399*, 704−708.
12. Sun, L., Zhang, K., Zhou, L., Hohler, P., Kool, E. T., Yuan, F., Wang, Z., and Taylor, J. S. (2003) Yeast Pol η Holds a Cis-Syn Thymine Dimer Loosely in the Active Site during Elongation Opposite the 3′-T of the Dimer, but Tightly Opposite the 5′-T, *Biochemistry 42*, 9431−9437.
13. Guckian, K. M., Schweitzer, B. A., Ren, R. X. F., Sheils, C. J., Paris, P. L., and Kool, E. T. (1996) Experimental Measurement of Aromatic Stacking Affinities in the Context of Duplex DNA, *J. Am. Chem. Soc. 118*, 8182−8183.
14. Guckian, K. M., Schweitzer, B. A., Ren, R. X. F., Sheils, C. J., Tahmassebi, D. C., and Kool, E. T. (2000) Factors Contributing to Aromatic Stacking in Water: Evaluation in the Context of DNA, *J. Am. Chem. Soc. 122*, 2213−2222.
15. Washington, M. T., Helquist, S. A., Kool, E. T., Prakash, L., and Prakash, S. (2003) Requirement of Watson−Crick hydrogen bonding for DNA synthesis by yeast DNA polymerase η, *Mol. Cell. Biol. 23*, 5107−5112.
16. Ling, H., Boudsocq, F., Plosky, B. S., Woodgate, R., and Yang, W. (2003) Replication of a cis-syn thymine dimer at atomic resolution, *Nature 424*, 1083−1087.
17. Nair, D. T., Johnson, R. E., Prakash, S., Prakash, L., and Aggarwal, A. K. (2004) Replication by human DNA polymerase-ι occurs by Hoogsteen base pairing, *Nature 430*, 377−380.
18. Washington, M. T., Johnson, R. E., Prakash, L., and Prakash, S. (2004) Human DNA polymerase ι utilizes different nucleotide incorporation mechanisms dependent upon the template base, *Mol. Cell. Biol. 24*, 936−943.
19. Cannistraro, V. J., and Taylor, J. S. (2004) DNA-Thumb Interactions and Processivity of T7 DNA Polymerase in Comparison to Yeast Polymerase η, *J. Biol. Chem. 279*, 18288−18295.
20. Taylor, J.-S., Brockie, I. R., and O'Day, C. L. (1987) A building block for the sequence-specific introduction of cis-syn thymine dimers into oligonucleotides. Solid-phase synthesis of TpT[c,s]pTpT, *J. Am. Chem. Soc. 109*, 6735−6742.
21. Taylor, J.-S., and Nadji, S. (1991) Unraveling the origin of the major mutation induced by ultraviolet light, the C-T transition at dTpdC sites. A DNA synthesis building block for the cis-syn cyclobutane dimer of dTpdU, *Tetrahedron 47*, 2579−2590.
22. Bloom, L. B., Otto, M. R., Beechem, J. M., and Goodman, M. F. (1993) Influence of 5′-nearest neighbors on the insertion kinetics of the fluorescent nucleotide analog 2-aminopurine by Klenow fragment, *Biochemistry 32*, 11247−11258.
23. Park, H., Zhang, K., Ren, Y., Nadji, S., Sinha, N., Taylor, J. S., and Kang, C. (2002) Crystal structure of a DNA decamer containing a cis-syn thymine dimer, *Proc. Natl. Acad. Sci. U.S.A. 99*, 15965−15970.
24. Kuchta, R. D., Mizrahi, V., Benkovic, P. A., Johnson, K. A., and Benkovic, S. J. (1987) Kinetic mechanism of DNA polymerase I (Klenow), *Biochemistry 26*, 8410−8417.
25. Minnick, D. T., Liu, L., Grindley, N. D., Kunkel, T. A., and Joyce, C. M. (2002) Discrimination against purine-pyrimidine mispairs in the polymerase active site of DNA polymerase I: A structural explanation, *Proc. Natl. Acad. Sci. U.S.A. 99*, 1194−1199.
26. Hwang, H., and Taylor, J. S. (2004) Role of base stacking and sequence context in the inhibition of yeast DNA polymerase η by pyrene nucleotide, *Biochemistry 43*, 14612−14623.
27. Washington, M. T., Johnson, R. E., Prakash, S., and Prakash, L. (1999) Fidelity and processivity of *Saccharomyces cerevisiae* DNA polymerase eta, *J. Biol. Chem. 274*, 36835−36838.
28. Cordonnier, A. M., and Fuchs, R. P. (1999) Replication of damaged DNA: Molecular defect in xeroderma pigmentosum variant cells, *Mutat. Res. 435*, 111−119.
29. Goodman, M. F., and Tippin, B. (2000) The expanding polymerase universe, *Nat. Rev. Mol. Cell Biol. 1*, 101−109.
30. Livneh, Z. (2001) DNA damage control by novel DNA polymerases: Translesion replication and mutagenesis, *J. Biol. Chem. 276*, 25639−25642.
31. Wang, Z. (2001) Translesion synthesis by the UmuC family of DNA polymerases, *Mutat. Res. 486*, 59−70.
32. Woodgate, R. (1999) A plethora of lesion-replicating DNA polymerases, *Genes Dev. 13*, 2191−2195.
33. Friedberg, E. C., and Gerlach, V. L. (1999) Novel DNA polymerases offer clues to the molecular basis of mutagenesis, *Cell 98*, 413−416.
34. Washington, M. T., Johnson, R. E., Prakash, S., and Prakash, L. (2000) Accuracy of thymine-thymine dimer bypass by *Saccharomyces cerevisiae* DNA polymerase η, *Proc. Natl. Acad. Sci. U.S.A. 97*, 3094−3099.
35. Johnson, R. E., Prakash, S., and Prakash, L. (1999) Efficient bypass of a thymine-thymine dimer by yeast DNA polymerase, Pol η, *Science 283*, 1001−1004.
36. Masutani, C., Araki, M., Yamada, A., Kusumoto, R., Nogimori, T., Maekawa, T., Iwai, S., and Hanaoka, F. (1999) Xeroderma pigmentosum variant (XP-V) correcting protein from HeLa cells has a thymine dimer bypass DNA polymerase activity, *EMBO J. 18*, 3491−3501.
37. Johnson, R. E., Kondratick, C. M., Prakash, S., and Prakash, L. (1999) hRAD30 mutations in the variant form of xeroderma pigmentosum, *Science 285*, 263−265.
38. Masutani, C., Kusumoto, R., Yamada, A., Dohmae, N., Yokoi, M., Yuasa, M., Araki, M., Iwai, S., Takio, K., and Hanaoka, F. (1999) The XPV (xeroderma pigmentosum variant) gene encodes human DNA polymerase η, *Nature 399*, 700−704.
39. Matsuda, T., Bebenek, K., Masutani, C., Hanaoka, F., and Kunkel, T. A. (2000) Low fidelity DNA synthesis by human DNA polymerase η, *Nature 404*, 1011−1013.
40. McDonald, J. P., Tissier, A., Frank, E. G., Iwai, S., Hanaoka, F., and Woodgate, R. (2001) DNA polymerase ι and related rad30-like enzymes, *Philos. Trans. R. Soc. London, Ser. B 356*, 53−60.
41. Kunkel, T. A., Pavlov, Y. I., and Bebenek, K. (2003) Functions of human DNA polymerases η, κ and ι suggested by their

properties, including fidelity with undamaged DNA templates, *DNA Repair 2*, 135−149.
42. Ling, H., Boudsocq, F., Woodgate, R., and Yang, W. (2001) Crystal structure of a Y-family DNA polymerase in action: A mechanism for error-prone and lesion-bypass replication, *Cell 107*, 91−102.
43. Trincao, J., Johnson, R. E., Escalante, C. R., Prakash, S., Prakash, L., and Aggarwal, A. K. (2001) Structure of the catalytic core of *S. cerevisiae* DNA polymerase *η*: Implications for translesion DNA synthesis, *Mol. Cell 8*, 417−426.
44. Kool, E. T. (2002) Active site tightness and substrate fit in DNA replication, *Annu. Rev. Biochem. 71*, 191−219.
45. Kool, E. T. (2001) Hydrogen bonding, base stacking, and steric effects in dna replication, *Annu. Rev. Biophys. Biomol. Struct. 30*, 1−22.
46. Fasman, G. D. (1975) *CRC Handbook of Biochemistry and Molecular Biology*, 3rd ed., Vol. I, CRC Press, Cleveland, OH.
47. Howard, F. B., Chen, C. W., Cohen, J. S., and Miles, H. T. (1984) Poly(d2NH2A-dT): Effect of 2-amino substituent on the B to Z transition, *Biochem. Biophys. Res. Commun. 118*, 848−853.
48. Scheit, K. H., and Rackwitz, H. R. (1982) Synthesis and physicochemical properties of two analogs of poly(dA): Poly(2-aminopurine-9-*β*-D-deoxyribonucleotide) and poly(2-aminodeoxyadenylic acid), *Nucleic Acids Res. 10*, 4059−4069.
49. Cheong, C., Tinoco, I., Jr., and Chollet, A. (1988) Thermodynamic studies of base pairing involving 2,6-diaminopurine, *Nucleic Acids Res. 16*, 5115−5122.
50. Moran, S., Ren, R. X. F., Rumney, S. I. V., and Kool, E. T. (1997) Difluorotoluene, a Nonpolar Isostere for Thymine, Codes Specifically and Efficiently for Adenine in DNA Replication, *J. Am. Chem. Soc. 119*, 2056−2057.
51. Ling, H., Boudsocq, F., Plosky, B. S., Woodgate, R., and Yang, W. (2003) Replication of a cis-syn thymine dimer at atomic resolution, *Nature 424*, 1083−1087.
52. McCulloch, S. D., Kokoska, R. J., Masutani, C., Iwai, S., Hanaoka, F., and Kunkel, T. A. (2004) Preferential cis-syn thymine dimer bypass by DNA polymerase *η* occurs with biased fidelity, *Nature 428*, 97−100.
53. Kemmink, J., Boelens, R., Koning, T., van der Marel, G. A., van Boom, J. H., and Kaptein, R. (1987) ^{1}H NMR study of the exchangeable protons of the duplex d(GCGT[]TGCG)-d(CGCAACGC) containing a thymine photodimer, *Nucleic Acids Res. 15*, 4645−4653.
54. Kim, J.-K., Patel, D., and Choi, B.-S. (1995) Contrasting structural impacts induced by cis-syn cyclobutane dimer and (6−4) adduct in DNA duplex decamers: Implication in mutagenesis and repair activity, *Photochem. Photobiol. 62*, 44−50.
55. McAteer, K., Jing, J., Kao, J., Taylor, J. S., and Kennedy, M. A. (1998) Solution-state structure of a DNA dodecamer duplex containing a cis-syn thymine cyclobutane dimer, the major UV photoproduct of DNA, *J. Mol. Biol. 282*, 1013−1032.
56. Sun, L., Wang, M., Kool, E. T., and Taylor, J. S. (2000) Pyrene Nucleotide as a Mechanistic Probe: Evidence for a Transient Abasic Site-Like Intermediate in the Bypass of Dipyrimidine Photoproducts by T7 DNA Polymerase, *Biochemistry 39*, 14603−14610.

BI048244+